Dinuclear Cu^{II} Complexes with a New Phenol-Based Ligand Bearing Pyridine and Thiophene Substituents: Synthesis, Characterization and Interaction with Catechol Substrates

Iryna A. Koval,[a] Mieke Huisman,[a] Arno F. Stassen,[a] Patrick Gamez,[a] Olivier Roubeau,[b] Catherine Belle,*[c] Jean-Louis Pierre,[c] Eric Saint-Aman,[d] Matthias Lüken,[e] Bernt Krebs,[e] Martin Lutz,[f] Anthony L. Spek,[f] and Jan Reedijk*[a]

Keywords: Copper / Dinuclear complexes / Catechol oxidase / Magnetochemistry / Electrochemistry

The reaction of the phenol-based ligand 4-methyl-2,6-bis{[(2-methylpyridyl)(2-methylthiophenyl)amino]methyl}phenol-(Hpy2th2s), containing pyridine and thiophene substituents, with copper(II) chloride and bromide yields two new dinuclear complexes with the composition $[Cu_2(py2th2s)X_3]$, where X = Cl or Br. In both complexes, the copper(II) ions are pentacoordinate and bridged by the deprotonated phenolate anion and by one halogen anion. Both complexes exhibit geometric asymmetry, as the coordination environment around one of the two copper ions is square-pyramidal, whereas the geometry around the other can be best described as a distorted trigonal bipyramid. The complexes were characterized by means of X-ray single-crystal diffraction, ligand field and EPR spectroscopy, mass spectrometry, and electrochemically. Magnetic susceptibility measurements indicate an antiferromagnetic coupling between the two metal centers ($2J \approx -200$ cm^{-1}). The interaction of the complexes with model substrates 3,5-di-*tert*-butylcatechol and tetrachlorocatechol is reported.

Introduction

The copper-containing proteins with a type-3 active site, e.g. hemocyanin, tyrosinase and catechol oxidase, have the ability to reversibly bind and activate dioxygen at ambient conditions.[1] For this reason, modeling of the active site of these proteins has attracted significant scientific interest during the last few decades.[2−8] Hemocyanin functions as a dioxygen-carrier protein in some mollusks and arthropods, whereas tyrosinase and catechol oxidase utilize dioxygen to perform selective oxidation of various organic substrates. Tyrosinase catalyzes the hydroxylation of tyrosine to dopa [3-(3,4-dihydroxyphenyl)alanine] (cresolase activity) and its subsequent oxidation to dopaquinone (catecholase activity), the initial steps in melanin biosynthesis. Catechol oxidase lacks the cresolase activity of tyrosinase and only catalyzes the aerial oxidation of *o*-diphenols to the corresponding *o*-diquinones.

The crystal structure of catechol oxidase has been determined in 1998 by Krebs and co-workers.[9] Its active site is characterized by a dinuclear copper center, in which each copper ion is surrounded by nitrogen donor atoms of three histidine residues from a protein backbone. A catalytic cycle for catechol oxidase activity has been proposed from a combination of biochemical, spectroscopic, and structural data[10] and by comparison with the tyrosinase-related cycle.[1] It begins with the interaction of the catechol substrate with the met form of the enzyme, which contains two copper(II) ions singly bridged by a hydroxo group, resulting in the formation of a stoichiometric amount of the quinone.

Dinucleating phenol-based compartmental ligands have been previously successfully applied to model the type-3 active site.[6,7,11,12] Recent studies on the copper complexes of H-BPMP ligand, published by some of us,[7] allowed to propose a new catalytic mechanism, emphasizing the role of the μ-hydroxo bridge between the two metal centers. It includes the monodentate coordination of the substrate to one of the metal centers with the concomitant cleavage of the OH bridge, and the subsequent proton transfer from

[a] Leiden Institute of Chemistry, Leiden University,
P. O. Box 9502, 2300 RA Leiden, The Netherlands
Fax: (internat.) + 31-71-527-42-61
E-mail: reedijk@chem.leidenuniv.nl
[b] Centre de Recherche Paul Pascal − CNRS UPR 8641,
115 avenue du Dr. A. Schweitzer, 33600 Pessac, France
[c] LEDSS, Chimie Biomimétique, UMR CNRS 5616, Université J. Fourier,
B. P. 53, 38041 Grenoble Cedex, France
E-mail: Catherine.Belle@ujf-grenoble.fr
[d] Laboratoire d'Electrochimie Organique et de Photochimie Redox, UMR CNRS 5630, Université J. Fourier,
B. P. 53, 38041 Grenoble Cedex, France
[e] Institut für Anorganische und Analytische Chemie der Westfälischen Wilhelms-Universität Münster,
Wilhelm-Klemm-Strasse 8, 48149 Münster, Germany
[f] Bijvoet Center for Biomolecular Research, Crystal and Structural Chemistry, Utrecht University,
Padualaan 8, 3584 CH Utrecht, Netherlands

the second OH group of the catechol substrate to the hydroxy group bound to the second copper center.[7] The release of a water molecule results in a bridging coordination of the catecholate, which undergoes an oxidation to quinone. In order to further demonstrate the importance of a μ-hydroxo bridge on the catalytic cycle, we report the synthesis of two dinuclear copper(II) chloride and bromide complexes with the new phenol-based ligand 4-methyl-2,6-bis[[(2-methylpyridyl)(2-methylthiophenyl)amino]methyl}phenol (abbreviated as Hpy2th2s), their structural, spectroscopic, magnetic and electrochemical properties, and their interaction with the model substrates 3,5-di-*tert*-butylcatechol (3,5-DTBC) and tetrachlorocatechol (TCC). In these complexes, the two metal ions are doubly bridged by the oxygen atom of the phenolate group and a halogen anion. It can be expected that the substitution of the μ-hydroxo group by a halogen anion should hamper the cleavage of the bridge and the subsequent proton transfer, thereby preventing the coordination of the catecholate in the bridging bidentate fashion, and thus hampering the catalytic cycle.

Results and Discussion

Synthesis

An interesting structural feature encountered in the active site of catechol oxidase from sweet potatoes (*Ipomoea batatas*)[9] and in active sites of some hemocyanins[13,14] is an unusual thioether bond between a carbon atom of one of the histidine ligands and the sulfur atom of a nearby cysteine residue from the protein backbone. There is also sequence homology evidence for this type of bridge in tyrosinase from *Neurospora crassa*.[15] Such a moiety was also encountered in the mononuclear copper enzyme galactose oxidase, in which it was proposed to stabilize the tyrosine radical generated during catalysis. However, the absence of this bridge in hemocyanins of arthropods and in human tyrosinase does not support the hypothesis about its direct involvement in the electron transfer process.[9]

Although a very large number of synthetic models of the type-3 active site appeared in the literature in the past few decades, relatively little attention has been paid to this thioether bond. In an attempt to mimic this quite unusual structural feature we prepared a new dinucleating phenol-based ligand Hpy2th2s with two pendant arms, containing pyridine and thiophene residues. The synthesis of this ligand is depicted in Figure 1.

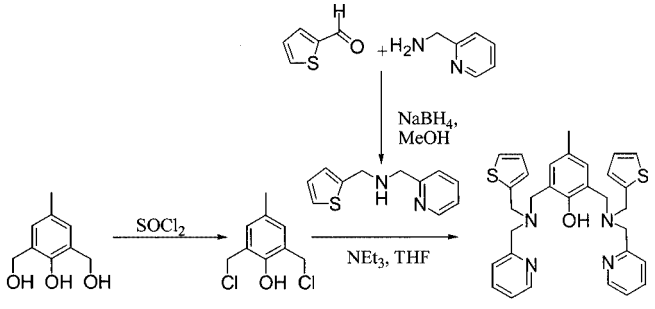

Figure 1. Reaction scheme of the synthesis of the ligand Hpy2th2s

The starting compound for the ligand synthesis, (2-picolyl)(2-thiophenyl)amine, was prepared by reaction of the commercially available 2-formylthiophene and (pyridin-2-ylmethyl)amine, followed by the reduction of the in situ generated imine by $NaBH_4$. Another starting compound 2,6-bis(chloromethyl)-4-methylphenol was prepared as described previously.[16] The reaction of 2,6-bis(chloromethyl)-4-methylphenol with a stoichiometric amount of (2-picolyl)(2-thiophenyl)amine in the presence of excess NEt_3 resulted in the formation of the ligand, which was isolated as a transparent light yellow oil. The reaction of Hpy2th2s with copper(II) chloride and bromide led to the formation of two new dinuclear copper complexes, which were isolated as dark brown and dark purple crystals, respectively.

Characterization of the Complexes

Crystal Structure Descriptions

[Cu_2(py2th2s)Cl_3]·CH_3OH (1)

Rectangular reddish-brown crystals of complex **1** were obtained by diethyl ether diffusion into a methanol solution containing stoichiometric amounts of copper(II) chloride and the ligand. A Platon[17] projection of the crystal structure of the complex is shown in Figure 2. Selected bond lengths and angles are presented in Table 1. The complex crystallizes as methanol solvate in space group $P2_1/n$ with four formula units present per unit cell. The dinuclear core is composed of two copper(II) ions, bridged on the one side by the endogenous cresolato bridge and on the other side by the chloride anion. The Cu···Cu separation in the complex is 3.185(1) Å. Both copper(II) ions are pentacoordinate with an identical N_2OCl_2 donor sets. However, the complex possesses geometrical asymmetry, as the coordination geometry around Cu1 is almost a regular square pyramid (τ = 0.10),[18] whereas the coordination environment around the Cu2 ion can be best described as a heavily distorted trigonal bipyramid (τ = 0.63).[18] The basal plane of the square pyramid around the Cu1 ion is made up of the nitrogen atom N1 of the tertiary amine group, the N2 atom of the pyridine ring, the oxygen atom O1 of the cresolate moiety, and the bridging chloride atom Cl1, whereas another chloride anion Cl2 occupies the apical position. In the case of the Cu2 ion, the nitrogen atom N3 of the tertiary amine group, the bridging chloride anion Cl1, and the chloride anion Cl3 form the equatorial plane of the trigonal bipyramid. The axial positions are occupied by the nitrogen atom N4 of the pyridine ring and the oxygen atom O1 of the cresolate group. The thiophene rings of the ligand remain noncoordinated; the Cu···S separations are > 5 Å. One of the thiophene rings shows disorder; the sulfur atom is refined on two independent positions, with occupancy factors of 78% (S1) and 22% (S1a). One noncoordinated disordered

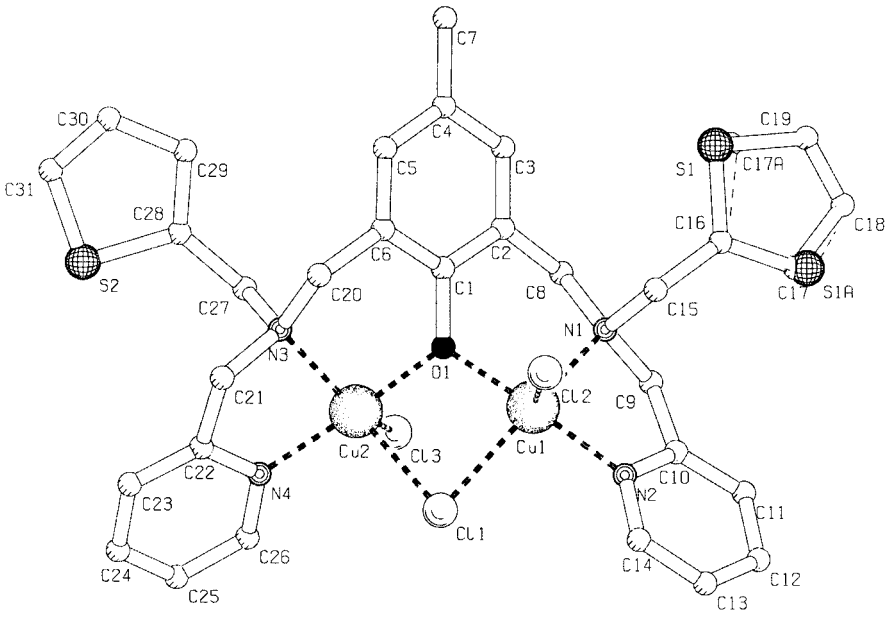

Figure 2. Platon[17] projection of the crystal structure $[Cu_2(py2th2s)Cl_3]\cdot CH_3OH$; hydrogen atoms and noncoordinated solvent molecule are omitted for clarity

Table 1. Selected bond lengths and bond angles of the complex $[Cu_2(py2th2s)Cl_3]\cdot CH_3OH$ (**1**)

Bond lengths [Å]			
Cu1−O1	1.9209(19)	Cu2−O1	1.911(2)
Cu1−N2	1.975(2)	Cu2−N4	1.972(2)
Cu1−N1	2.103(2)	Cu2−N3	2.083(2)
Cu1−Cl1	2.3922(8)	Cu2−Cl1	2.4717(9)
Cu1−Cl2	2.3931(10)	Cu2−Cl3	2.3636(10)
Cu1−Cu2	3.185(1)		
Bond angles [°]			
O1−Cu1−N2	159.33(9)	O1−Cu2−N4	168.80(9)
O1Cu1−N1	90.47(8)	O1−Cu2−N3	90.59(8)
N2−Cu1−N1	81.53(9)	N4−Cu2−N3	82.01(9)
O1−Cu1−Cl1	82.70(6)	O1−Cu2−Cl1	80.76(6)
N2−Cu1−Cl1	95.90(7)	N4−Cu2−Cl1	97.76(7)
N1−Cu1−Cl1	153.25(6)	N3−Cu2−Cl1	131.18(6)
O1−Cu1−Cl2	100.79(7)	O1−Cu2−Cl3	94.77(7)
N2−Cu1−Cl2	99.74(7)	N4−Cu2−Cl3	96.43(7)
N1−Cu1−Cl2	106.18(6)	N3−Cu2−Cl3	130.53(6)
Cl1−Cu1−Cl2	100.50(3)	Cl1−Cu2−Cl3	98.17(4)

methanol molecule is present per formula unit, which is hydrogen-bonded to the chloride anion Cl3.

[Cu₂(py2th2s)Br₃] (2)

Very dark purple needles of complex **2** were obtained by slow concentration of an acetonitrile solution containing stoichiometric amounts of copper(II) bromide and the ligand. A Platon[17] projection of the crystal structure is shown in Figure 3. Selected bond lengths and angles are presented in Table 2. The complex crystallizes in space group $P\bar{1}$. The asymmetric unit consists of two independent formula units. As in the case of the chloride complex **1**, two copper(II) ions are doubly bridged by the oxygen atom of the cresolate moiety and the halogen anion. The Cu···Cu distances are 3.2710(10) and 3.2394(10) Å, respectively. The copper ions are pentacoordinate, with N_2OBr_2 donor sets. One of the two independent formula units (Cu11, Cu12) possesses geometrical asymmetry. The geometry around the Cu11 ion is a slightly distorted square pyramid (τ = 0.17),[18] whereas the geometry around the Cu12 ion is a very distorted trigonal bipyramid (τ = 0.58).[18] The nitrogen atom N11 of the tertiary amine group, the nitrogen atom N12 of the pyridine ring, the bridging oxygen atom O11, and the bridging bromide anion Br11 form the basal plane of the square pyramid around the Cu11 ion, whereas the monocoordinated bromide anion Br12 occupies the axial position. The equatorial plane of the trigonal bipyramid around the Cu12 ion is formed by the nitrogen atom N13 of the tertiary amine group and the bromide atoms Br11 and Br13. The axial positions of the bipyramid are occupied by the bridging oxygen atom of the cresolate group and the nitrogen atom N14 of the pyridine ring. One of the noncoordinated thiophene rings is rotationally disordered. Thus, the first orientation has an occupancy factor of 85%, while the 180° rotated orientation has an occupancy factor of 15%.

In the second independent formula unit, both copper(II) ions (Cu21 and Cu22) have significantly distorted square-pyramidal surroundings (τ = 0.26 for the Cu21 ion and 0.45 for the Cu22 ion)[18]. The basal plane around the Cu21 ion is made up of, as in the case of the Cu11 ion, the two nitrogen atoms N21 and N22, the oxygen atom O21 of the cresolate group, and the bridging halogen atom Br21, whereas the bromide anion Br22 occupies the apical position. For the Cu22 ion, the nitrogen atom N23 of the ter-

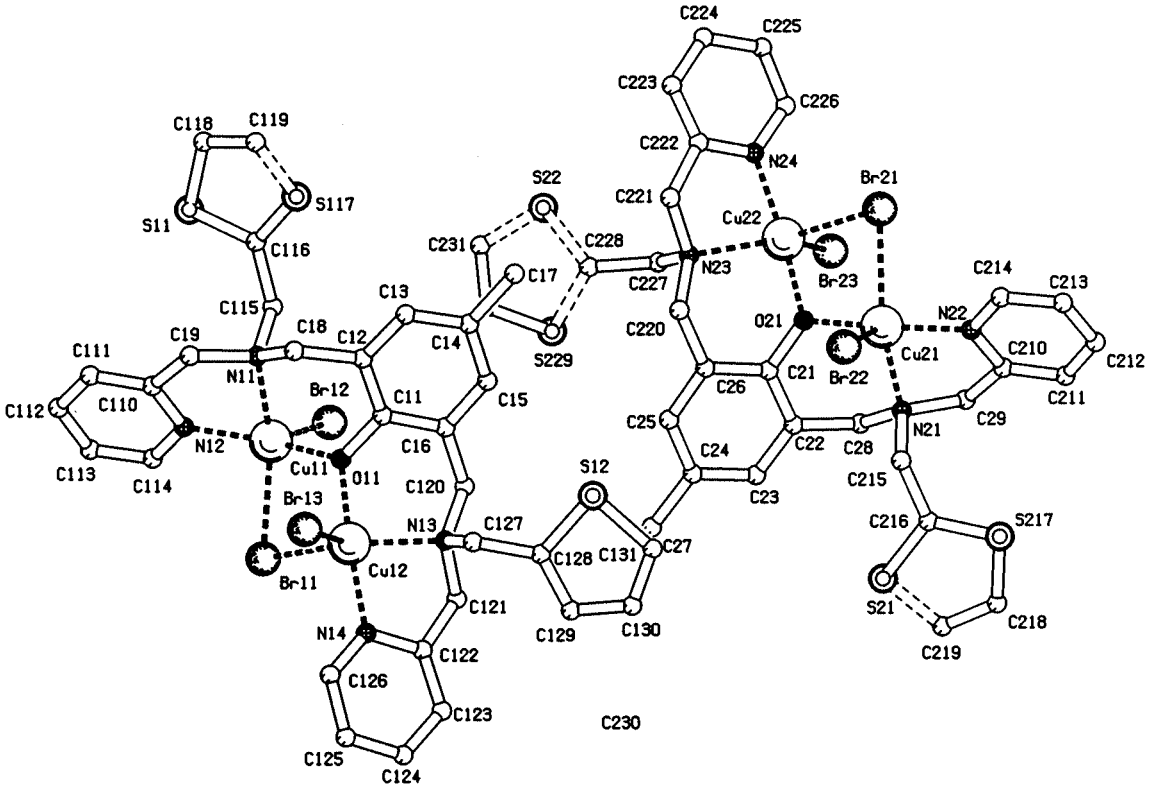

Figure 3. Platon[17] projection of the two independent formula units of $[Cu_2(py2th2s)Br_3]$; hydrogen atoms are omitted for clarity; three of the thiophene rings are rotationally disordered

tiary amine group, the nitrogen atom N24, the bridging oxygen atom O21, and the bridging bromide anion Br21 form the basal plane of the square pyramid, and its apical position is occupied by the Br23 atom. Thus, two square pyramids share one side through the atoms O21 and Br21, with their apical positions *trans*-located to each other. Both thiophene rings of the ligand remain noncoordinated (Cu···S separations are > 5 Å) and exhibit rotational disorder. Thus, the thiophene ring at S21 was refined on two orientations with occupancies of 0.72 and 0.28, respectively, and the thiophene ring at S22 with occupancies of 0.55 and 0.45, respectively.

Physical Methods

Ligand Field Spectroscopy

The ligand field spectra of both complexes, recorded in the solid state (diffuse reflectance), exhibit almost identical features. Both spectra are characterized by the presence of the charge-transfer band from the phenolate moiety to the copper ions[11] around 500 nm (483 nm for complex **1** and 521 nm for complex **2**) and the d-d transition band of the copper(II) ions. The latter band, observed at 774 nm for the chloride complex and at 806 nm for the bromide complex, is asymmetric in both cases, with a shoulder observed at higher wavelengths. As shown previously, such spectroscopic behavior (high-energy absorption band in the visible region with a low-energy shoulder) is typical for square-pyramidal copper(II) complexes.[19] In acetonitrile solution, the charge-transfer band is observed at 472 nm for complex **1** (ε = 1851 $M^{-1}\cdot cm^{-1}$) and at 500 nm for complex **2** (ε = 1812 $M^{-1}\cdot cm^{-1}$). The d-d band is located at 771 nm (ε = 464 $M^{-1}\cdot cm^{-1}$) for complex **1** and 791 nm (ε = 534 $M^{-1}\cdot cm^{-1}$) for complex **2**. A small shift of the d-d bands upon dissolution of the complexes in acetonitrile may suggest the coordination of the solvent to the metal centers. However, the partial dissociation of the complexes due to the exchange of the halide anions with acetonitrile molecules can also not be excluded.

EPR and Magnetic Susceptibility Studies

Both complexes **1** and **2** are EPR-silent in the solid state and in a frozen acetonitrile solution at 100 K, suggesting an antiferromagnetic coupling between the copper ions. Such a behavior is confirmed by the temperature dependence of the molar magnetic susceptibility χ_M depicted in Figure 4, which is typical for complexes of antiferromagnetically coupled copper(II) dimers. Indeed the χ_M vs. T curves present a broad maximum centered around 160 and 190 K for **1** and **2**, respectively, while the values of χ_M at high temperatures (2.10×10^{-3} and 1.85×10^{-3} $cm^3\cdot mol^{-1}$ at 300 K, respectively) are slightly lower than expected for two uncoupled copper(II) ions (2.5×10^{-3} $cm^3\cdot mol^{-1}$ for g = 2). Below 40 K, a Curie tail ascribed to paramagnetic impurity is observed, which is usual in such copper(II) complexes. These experimental data were reproduced correctly using

Table 2. Selected bond lengths and bond angles of the complex $[Cu_2(py2th2s)Br_3]$ (**2**)

Bond lengths [Å]			
Cu11−O11	1.925(3)	Cu12−O11	1.931(4)
Cu11−N12	1.977(4)	Cu12−N14	1.986(5)
Cu11−N11	2.099(4)	Cu12−N13	2.096(4)
Cu11−Br11	2.5620(9)	Cu12−Br11	2.5226(8)
Cu11−Br12	2.5314(8)	Cu12−Br13	2.4870(9)
Cu21−O21	1.931(3)	Cu22−O21	1.918(4)
Cu21−N22	1.968(4)	Cu22−N24	1.981(5)
Cu21−N21	2.112(4)	Cu22−N23	2.113(4)
Cu21−Br21	2.5535(10)	Cu22−Br21	2.5666(9)
Cu21−Br22	2.5166(9)	Cu22−Br23	2.4953(9)
Cu11−Cu12	3.2710(10)	Cu21−Cu22	3.2394(10)
Bond angles [°]			
O11−Cu11−N12	159.37(17)	O11−Cu12−N14	165.93(17)
O11−Cu11−N11	91.14(16)	O11−Cu12−N13	91.70(17)
N11−Cu11−N12	81.55(17)	N13−Cu12−N14	81.61(19)
Br11−Cu11−O11	81.00(11)	Br11−Cu12−O11	81.95(10)
Br11−Cu11−N12	95.53(13)	Br11−Cu12−N14	93.07(13)
Br11−Cu11−N11	149.47(13)	Br11−Cu12−N13	130.96(12)
Br12−Cu11−O11	97.77(11)	Br13−Cu12−O11	96.52(11)
Br12−Cu11−N12	102.84(12)	Br13−Cu12−N14	97.54(13)
Br12−Cu11−N11	108.72(13)	Br13−Cu12−N13	119.60(12)
Br11−Cu11−Br12	101.58(3)	Br11−Cu12−Br13	109.44(3)
O21−Cu21−N22	162.14(18)	O21−Cu22−N24	164.78(18)
O21−Cu21−N21	91.15(16)	O21−Cu22−N23	90.99(17)
N21−Cu21−N22	81.54(17)	N23−Cu22−N24	81.71(19)
Br21−Cu21−O21	83.16(12)	Br21−Cu22−O21	83.04(11)
Br21−Cu21−N22	93.90(14)	Br21−Cu22−N24	93.39(15)
Br21−Cu21−N21	146.37(13)	Br21−Cu22−N23	137.81(12)
Br22−Cu21−O21	99.57(12)	Br23−Cu22−O21	95.20(11)
Br22−Cu21−N22	98.26(13)	Br23−Cu22−N24	99.98(14)
Br22−Cu21−N21	110.29(13)	Br23−Cu22−N23	122.65(12)
Br21−Cu21−Br22	103.34(3)	Br21−Cu22−Br23	99.51(3)
Cu11−O11−Cu12	116.04(18)	Cu21−O21−Cu22	114.63(19)
Cu11−Br11−Cu12	80.08(3)	Cu21−Br21−Cu22	78.50(3)

the modified Bleaney−Bowers equation [Equation (1)], where χ_M is the magnetic susceptibility per dimer. In this equation, $2J$ corresponds to the singlet-triplet energy gap, ρ to the fraction of paramagnetic impurity, and TIP to a term to account for temperature-independent paramagnetism, while N_A, β, k_B, and g have their usual meaning. The paramagnetic impurity was assumed to be a mononuclear copper(II) species and g was fixed to 2. The best-fit parameters were then obtained as $2J = -177(2)$ cm^{-1}, ρ = 1.8(1)% and TIP = 2.9(1) × 10^{-4} cm^3·mol^{-1} for complex **1**, and $2J = -219(1)$ cm^{-1}, ρ = 0.6(1)% and TIP = 2.0(1) × 10^{-4} cm^3·mol^{-1} for complex **2**.

$$\chi_M = (1-\rho)\frac{2N_A\beta^2g^2}{k_BT}\left[3+\exp(-2J/k_BT)\right]^{-1} + 2\rho\left(\frac{N_A\beta^2}{k_BT}\right) + TIP \quad (1)$$

These medium antiferromagnetic couplings should be correlated to a significant overlap between the two magnetic orbitals of the two copper(II) ions in complexes **1** and **2**, through both the halide and phenolate bridges. The short

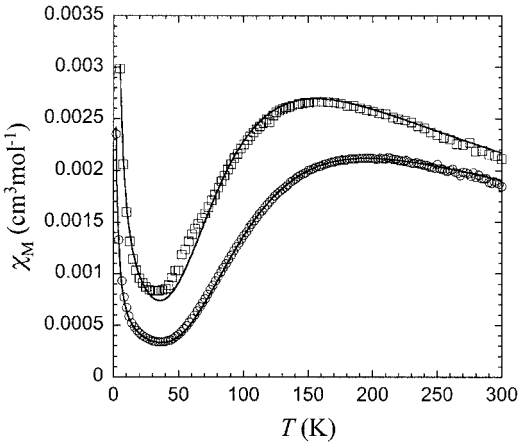

Figure 4. χ_M vs. T curve for complexes **1** (squares) and **2** (circles); see text for further details

Cu−O bonds and the large Cu−O−Cu angles of the phenolate bridge in **1** and **2**, relative to the long Cu−X bonds, point at a dominant coupling through the phenolate bridge. The coordination sphere around one of the two copper ions is intermediate between a square pyramid and a trigonal bipyramid, while the other has a square-pyramidal environment. In the former case, the unpaired electron of copper(II) occupies either the d_{z^2} or the $d_{x^2-y^2}$ orbital, which would both point along the Cu−O(phenolate) bond. Short Cu−O bonds and large Cu−O−Cu angles in square-pyramidal phenolate-bridged Cu dimers result in a strong overlap of $d_{x^2-y^2}$ orbitals and thus produce strong to very strong antiferromagnetic couplings.[20] On the other hand, if one of the copper ions in such dimers has a trigonal-bipyramidal environment, weaker overlap is expected, and even weak ferromagnetic coupling has been observed.[21,22] Therefore, the smaller singlet-triplet energy gap in **1** can be related to a smaller Cu−O−Cu angle in **1** (ca. 112°) relative to **2** (on average over the two dimeric units about 115.3°), but also to a more distorted trigonal-bipyramidal coordination sphere in **2** (τ = 0.58, Cu12) than in **1** (τ = 0.63, Cu2). Most likely, the difference in the singlet-triplet energy gap results from both structural differences.

Electrochemistry

The electrochemical behavior of both complexes was investigated by cyclic voltammetry (CV) and rotating disk electrode voltammetry (RDE) in acetonitrile solution, with tetra-*n*-butylammonium perchlorate (TBAP) as supporting electrolyte (0.1 M). The potentials were referred to an Ag/10 mM $AgNO_3$ + CH_3CN +0.1 M TBAP reference electrode.

When scanning towards the negative region of potentials, the CV curve for both complexes **1** and **2** is characterized by three successive electrochemical signals (Figures 5 and 6). The first signal for **1**, at $E_{pc} = -0.52$ V, is irreversible, and re-oxidation of the reduced species is seen on the reverse scan at +0.23 V (Figure 5, curve a), while that for **2** appears to be weakly reversible at $E_{1/2} = -0.34$ V (ΔE_p =

0.12 V, Figure 6, curve a). Coulometric titrations give n = 1 for the exchanged electron per complex, allowing to attribute this electrochemical process to the complexed $Cu_2^{II,II}/Cu_2^{II,I}$ redox couple. The UV/Vis spectra of the one-electron reduced complexes exhibit one very broad band around 680 nm. The lack of reversibility of the first electrochemical reduction of **1** and **2** suggests a change in the coordination sphere around the metal center upon reduction, likely a partial dissociation of the exogenous halide ligand and a change in the geometry of the coordination sphere. Additional electrochemical measurements performed at −40 °C showed that the course of these coupled chemical reactions is not prevented at low temperature. The second electrochemical signal, weakly reversible at $E_{1/2}$ = −0.78 V for **1** and at $E_{1/2}$ = −0.72 V for **2**, also corresponds to a one-electron process, leading to the complexed $Cu_2^{II,I}/Cu_2^{I,I}$ redox couple. Finally, the third electrochemical signal at E_{pc} = −1.45 V for **1** and −1.04 V for **2** corresponds to a two-electron process, suggesting the reduction of Cu^{I} ions to the Cu^0 state and the deposition of metallic copper on the electrode surface. Accordingly, an additional sharp anodic peak is observed on the reverse scan, which is caused by the redissolution of metallic copper.

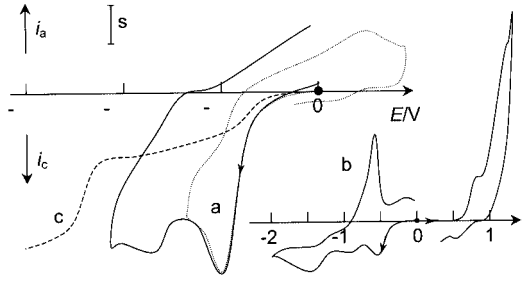

Figure 5. Electrochemical curves recorded in a 0.67 mM solution of **1** in CH_3CN + TBAP 0.1 M on a Pt disc [diameter = 5 (a, b) or 3 (c) mm]; curves a, b: CV curves, ν = 0.1 $V{\cdot}s^{-1}$; curve c: RDE curve, N = 600 rpm; V vs. $Ag/AgNO_3$ mM + CH_3CN + TBAP 0.1 M; scale s = 20 μA (curve a), 120 μA (curve b) or 10 μA (curve c)

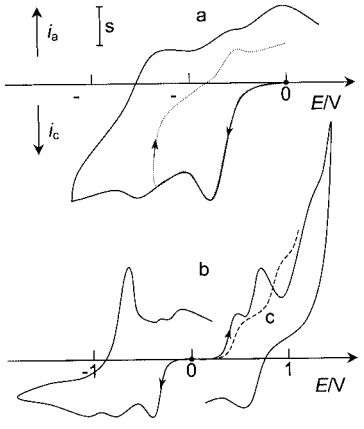

Figure 6. Electrochemical curves recorded in a 0.67 mM solution of **2** in CH_3CN + TBAP 0.1 M on a Pt disc [diameter = 5 (a, b) or 3 (c) mm]; curves a, b: CV curves, ν = 0.1 $V{\cdot}s^{-1}$; curve c: RDE curve, N = 600 rpm; V vs. $Ag/AgNO_3$ mM + CH_3CN + TBAP 0.1 M; scale s = 20 μA (curve a), 40 μA (curve b, c)

The anodic behavior of complexes **1** and **2** differs. The anodic part of the CV curve for **1** (Figure 5, b) is characterized by two electrochemical signals, whereas three signals are observed on the CV curve for **2** (Figure 6, b). For **1**, the first signal at $E_{1/2}$ = 0.64 V (ΔE_p = 0.26 V) corresponds to a one-electron quasi-reversible oxidation of **1**. The electron transfer is likely to be centered on the phenolate bridge, as previously shown for other phenolate-bridged dinuclear copper(II) complexes.[11,23] This process is followed by the oxidation of the chloride anions, which is seen as a shoulder at the negative foot of the over-oxidation wave of the complex (free chloride anions are reversibly oxidized at 0.72 V under our experimental conditions). The CV curve recorded in a solution of **2** shows an additional fully irreversible one-electron process at E_{pa} = 0.47 V. This is assumed to be due to the one-electron oxidation of bromide anions; free bromide anions are irreversibly oxidized at E_{pa} = 0.39 V under our experimental conditions. The one-electron phenolate-based oxidation of complex **2**, similarly to **1**, is observed as a quasi-reversible pair of peaks at $E_{1/2}$ = 0.76 V (ΔE_p = 0.18 V), and is followed at higher potentials by the over-oxidation of the complex.

These results have been confirmed by rotating disk electrode (RDE) voltammetric experiments (Figures 5 and 6). The RDE curves display one anodic wave at $E_{1/2}$ = 0.84 V for **1** and two successive well-behaved anodic waves at $E_{1/2}$ = 0.42 V and 0.82 V (Figure 6, curve c) for **2**. For both complexes, three successive cathodic waves are seen. For **1** and **2**, the first one at $E_{1/2}$ = −0.42 V and −0.40 V, respectively, is followed by a second ill-behaved wave at $E_{1/2}$ = −0.78 V and −0.80 V, respectively. The third cathodic wave corresponding to the deposition of metallic copper onto the electrode surface is observed at $E_{1/2}$ = −1.22 V and −1.20 V, respectively.

Conductivity Measurements

The conductivity measurements of the complexes **1** and **2** were performed on 0.5 mM solutions of the complexes in acetonitrile. The calculated values for equivalent conductivities of both compounds are roughly the same and are equal to 52 $cm^2{\cdot}mol^{-1}{\cdot}\Omega^{-1}$ for complex **1** and 55 $cm^2{\cdot}mol^{-1}{\cdot}\Omega^{-1}$ for complex **2**. Previously, the conductivity range for complexes corresponding to the 1:1-type electrolytes was suggested to lie between 120 and 160 $cm^2{\cdot}mol^{-1}{\cdot}\Omega^{-1}$ if acetonitrile was utilized as a solvent.[24] Although values as low as 90 $cm^2{\cdot}mol^{-1}{\cdot}\Omega^{-1}$ were also reported in some cases, the observed conductivities of both complexes **1** and **2** are still too low for them to be considered as 1:1 electrolytes. As shown previously,[25] such small conductivity values in acetonitrile are often found for nonelectrolytes, due to coordinating and solvating properties of this solvent. Some authors[25] argue that they may indicate a partial exchange of counter anions with the solvent molecules. Small changes in the positions of UV/Vis/NIR d-d bands of the complexes upon their dissolution in acetonitrile, observed in our case, appear to sustain this assumption.

Interaction of the Complexes with the Model Substrates

Catecholase Activity Measurements

To evaluate the ability of the complexes to behave as functional models of catechol oxidase, they were tested as catalysts in the oxidation of 3,5-di-*tert*-butylcatechol (3,5-DTBC), a widely used model substrate, to the respective quinone. Both complexes exhibit only negligible catecholase activity (TON $<$ 1 after 30 min), making a detailed kinetic analysis dispensable. These results are as expected, confirming that the substitution of the μ-hydroxo bridge by a halogen anion precludes catecholase activity. However, these results do not provide information on whether or not the binding of the substrate to the metal centers takes place *at all*. Reim et al. have previously shown that, in the case of essentially inactive complexes, no interaction between the dimetal core and the substrate occurred.[6] To evaluate whether or not the first step of the catalytic cycle, e.g. the binding of catechol to the metal centers, takes place, we studied the interaction of the complexes with tetrachlorocatechol (TCC). The latter catechol has a very high oxidation potential due to its electron-withdrawing substituents and is not oxidized by copper complexes.

TCC Binding Studies

The titration of 5×10^{-4} M solutions of the complexes in acetonitrile with TCC was monitored by means of UV/Vis and EPR spectroscopy. The changes observed in the UV/Vis spectra of complex **1** upon addition of TCC (up to 4 equiv.) are depicted in Figure 7. Quite significant changes in the spectrum of the original complex indicate the interaction between the substrate and the metal centers. The presence of two isosbestic points at 570 nm and 724 nm shows the presence of only two absorbing species in solution. The Cu^{II} d-d transition band shifts gradually from 789 nm to 718 nm, whereas its absorbance decreases to about 50% of its initial value. Also, the extinction coefficient of the LMCT band decreases from 1851 to about 1600 $M^{-1}\cdot cm^{-1}$ (Figure 7).

Whereas the chloride complex obviously reacts with TCC, no changes were observed in the UV/Vis spectrum upon addition of TCC to the bromide complex. Taking into account the great structural similarity between the two complexes, it seems reasonable to us to suggest that the difference in their behavior is caused by the different halogen anions coordinated to the copper ions. The Cu−Cl bond has a more ionic character than the Cu−Br bond, which facilitates the substitution of (at least one of) the chloride anions by catechol, whereas no exchange of Br anions by TCC occurs.

Titration of complex **1** with TCC, monitored by X-band EPR spectroscopy, revealed that no evolution of the EPR signal is observed upon addition of TCC. This indicates that the two copper ions are strongly antiferromagnetically coupled, suggesting that they probably remain doubly bridged by the phenolate group and the chloride anion. Although a few structures of copper(II) complexes with bridging catecholate were previously described,[8,26] no magnetic properties of these compounds have been reported. However, we believe that the cleavage of the halide bridge would lead to a decrease in strength of the magnetic coupling, similarly to the behavior seen in previously reported μ-hydroxo complexes with phenol-based ligands[7] after the cleavage of the hydroxo bridge. Thus, the reaction of TCC with the chloride complex probably results in the substitution of at least one of the apical chloride anions.

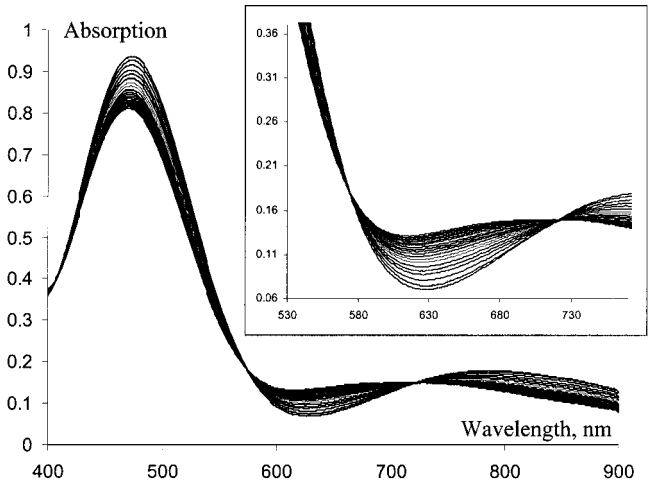

Figure 7. UV/Vis titration of complex **1** (0.5 mM solution in acetonitrile) with TCC (from 0 to 4 equiv.); the inset shows the enlargement of the spectroscopic curves in the range 530−780 nm

In order to further confirm this hypothesis, the conductivity of complex **1** in acetonitrile solution before and after addition of TCC was studied. The equivalent conductivity of TCC itself is negligible.

The values of the equivalent conductance observed after addition of 1−4 equiv. of TCC to 0.5 mM solution of complex **1** are listed in Table 3. As can be seen, a substantial increase is observed after 1 equiv. of TCC has been added. Further addition of TCC leads to a slight increase in conductivity, until a final value of 118 $cm^2\cdot mol^{-1}\cdot\Omega^{-1}$ is reached. This value fits perfectly in a range suggested for the 1:1 electrolytes in acetonitrile.[24] The interaction of **1** with TCC leads to the release of one chloride anion in solution; complete release is reached in the presence of an excess of TCC as shown by the slight increase in the conductivity above 1 mol-equiv. added. The reversible nature of this process is further confirmed by UV/Vis titration experiments

Table 3. Calculated values of equivalent conductivity upon treating 0.5 mM solution of **1** in acetonitrile with TCC

Number of equiv. of TCC	Equivalent conductivity [$cm^2\cdot mol^{-1}\cdot\Omega^{-1}$]
0	52
1	100
2	110
3	117
4	118

that showed that the maximal perturbation in the UV/Vis spectra was reached in the presence of at least 3 equiv. of TCC (Figures 7 and 8).

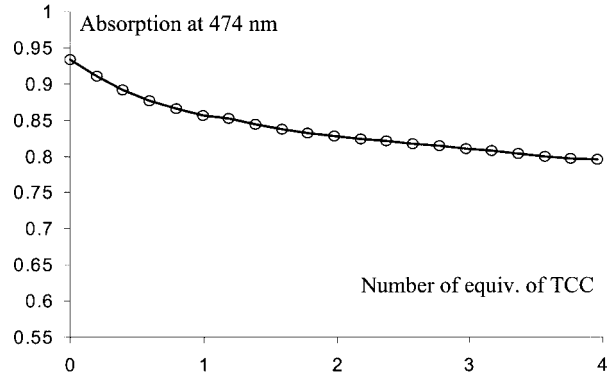

Figure 8. Decrease in the LMCT band (474 nm) upon titration of the solution of **1** (0.5 mM) in acetonitrile with TCC

Not surprisingly, additions of TCC to the bromide complex do not lead to an increase in conductivity, in complete agreement with the hypothesis that substitution of Br^- anions by TCC is not possible.

General Discussion

Previously, many attempts to establish a correlation between the structural parameters of the complexes and their catalytic activity in the oxidation of catechols were described in the literature. Three most important criteria influencing the catalytic properties of the complexes can now be distinguished: (i) the distance between the metal centers,[11,27,28] (ii) the nature of the bridging group between the metal ions,[29,30] (iii) the electronic properties of the complexes.[23] Some other factors, e.g. the imposed strain in the complex due to the rigidity of either the ligand and/or the bridging group, may also play a role.[6] Results published by Reim et al.[6] indicate that complexes with strained structures show catalytic activity, whereas complexes present in relaxed and energetically favored conformations are essentially inactive towards catechol oxidation. In the chloride and bromide complexes **1** and **2**, the metal−metal distance and the redox potentials of the metal ions are similar to the values previously determined for catalytically active complexes;[6,11,29] thus, the absence of catalytic activity is not likely to be due to these two factors. Also, the coordination spheres around the copper ions in both complexes exhibit quite a large distortion from a regular square-pyramidal geometry, resulting in relatively strained structures. Thus, the main reason for the absence of catalytic activity lies in the nature of the bridging groups between the two copper ions in the complexes. As discussed above, the crucial steps of the mechanism that was proposed earlier[7] is the cleavage of the OH bridge between the two metal ions and the subsequent proton transfer from the catechol substrate to the hydroxy anion, leading to the release of one water molecule. We have shown that the reaction of catechol with the complexes **1** and **2** does not result in a cleavage of the bridge, although binding of the substrate to the chloride complex undoubtedly takes place. These results thus emphasize the influence of the bridging group between the copper centers on the catecholase activity of the complexes and underline the importance of the exogenous hydroxo bridge for the catalytic mechanism. This hydroxo ligand appears to be the key factor to achieve the complete deprotonation of catechol, leading to a bridging catecholate prior to the electron transfer. Upon substitution of the hydroxo bridge with the halogen anion, no proton transfer can occur, precluding the binding of catecholate in a bidentate bridging fashion, and thus the subsequent catalytic cycle.

Conclusion

The synthesis of a new phenol-based ligand Hpy2th2s bearing thiophene- and pyridine-containing pendant arms was successfully accomplished. Two dinuclear copper(II) complexes with this ligand were isolated and characterized by means of single-crystal X-ray analysis, UV/Vis and EPR spectroscopy, magnetochemistry and electrochemistry. Both complexes were found to be essentially inactive in the catalytic oxidation of 3,5-di-*tert*-butylcatechol to the respective quinone. The presence of chloride and bromide anions as bridging ligands between the two metal centers precludes the deprotonation of catechol and its binding in a bidentate bridging fashion to the copper ions, and thus from further oxidation. Studies to establish a better structure-activity relationship for dinuclear copper(II) complexes as structural models of catechol oxidase are currently in progress.

Experimental Section

General Remarks: All starting materials were commercially available and used as purchased. 2,6-Bis(chloromethyl)-4-methylphenol was prepared as described previously.[16] The NMR spectra were recorded with a JEOL FX-200 (200 MHz) FT NMR spectrometer. The ligand field spectra of the solids (300−2000 cm^{-1}, diffuse reflectance) were taken with a Perkin−Elmer 330 spectrophotometer equipped with a data station. The ligand field spectra in solution were recorded with a Varian Cary 50 Scan UV/Vis spectrophotometer. Electrospray mass spectra (ESI-MS) in acetonitrile solutions were recorded with a Thermo Finnigan AQA apparatus. X-band electron paramagnetic resonance (EPR) measurements were performed at 77 K in the solid state with a Jeol RE2x electron spin resonance spectrometer, using DPPH (g = 2.0036) as a standard, and at 100 K as acetonitrile frozen solutions with a Bruker ESP 300E spectrometer operating at 9.4 GHz (X-band). The conductivity measurements were performed with a Philips PW9526 digital conductivity meter and PW 9552/60 measuring cell with 0.5 mM solutions of the complexes in acetonitrile. The electrochemical behavior of the complexes was investigated in a 0.1 M solution of tetra-*n*-butylammonium perchlorate (TBAP) in acetonitrile using an EGG 273 potentiostat coupled with a Kipp&Zonen *x*-*y* recorder. The experiments were performed at room temperature or at −40 °C in a three-compartment cell. Potentials are referred to

an Ag/10 mM $AgNO_3$ + CH_3CN +0.1 M TBAP reference electrode. The working electrode was a platinum disk with a 5 mm diameter for the cyclic voltammetry (CV, 0.1 V/s) experiments or 3 mm diameter for the rotating disk electrode (RDE, 600 rpm) voltammetry experiments. The working electrode was polished with 1 μm diamond paste prior to each recording. Bulk magnetizations of polycrystalline samples were performed on the crystals of complexes **1** (11.11 mg) and **2** (16.88 mg) in the temperature range 5−400 K with a Quantum Design MPMS-5S SQUID magnetometer in a 1 kG applied field. The data were corrected for the experimentally determined contribution of the sample holder. Corrections for the diamagnetic responses of the complexes, as estimated from Pascal's constants, were applied.[31]

Catecholase Activity Study: The catecholase activity of the complexes was evaluated by reaction with 3,5-di-*tert*-butylcatechol at 25 °C. The absorption at 400 nm, characteristic of the formed quinone, was measured as a function of time. The experiments were performed under 1 atm of dioxygen; 3 mL of $2.5 \cdot 10^{-4}$ M solution of complex in acetonitrile was placed in 1-cm path-length cell, and 75 μL of a 1 M solution of the substrate in the same solvent was added. After thorough shaking, the changes in UV/Vis spectra were recorded over 30 min. The titration of the complexes with tetrachlorocatechol (TCC) was carried out by adding 3 μL aliquots of 0.1 M solution of TCC (corresponding to 0.198 equiv. of TCC/1 equiv. of the complex) to 3 mL of 5×10^{-4} M solution of complex in acetonitrile.

(2-Picolyl)(2-thiophenyl)amine: A solution of (pyridin-2-ylmethyl)-amine (2.00 g, 18.5 mmol) was added dropwise, while stirring, to a solution of 2-formylthiophene (2.08 g, 18.5 mmol) in MeOH. The resulting solution was stirred at room temperature overnight. Afterwards, $NaBH_4$ (2.1 g, 56 mmol, 3 equiv. per 1 CH=N) was added slowly, and the resulting solution was heated at 50 °C for 3 h. After concentration, the obtained oil was redissolved in a mixture of dichloromethane and water. The organic and aqueous layers were separated, and the water layer was washed twice with a small amount of dichloromethane. After combining and drying of the dichloromethane layers with Na_2SO_4 and concentration, the pure product was obtained as a light yellow oil. The product is light-sensitive and should preferably be stored in darkness at low temperatures. Yield: 3.59 g (95%). ^{1}H NMR ($CDCl_3$): δ = 2.28 (s, 1 H, NH), 3.95 (s, 2 H, NHCH_2th), 4.03 (s, 2 H, NHCH_2py), 6.93 (d, 1 H, 3′th), 6.96 (s, 1 H, 4′th), 7.20 (d, 1 H, 5′th), 7.15 (t, 1 H, 5′py), 7.30 (d, 1 H, 3′py), 7.62 (t, 1 H, 4′py), 8.55 (d, 1 H, 6′py) ppm.

4-Methyl-2,6-bis{[(2-methylpyridyl)(2-methylthiophenyl)amino]-methyl}phenol (Hpy2th2s): A solution of (2-picolyl)(2-thiophenyl)-amine (0.7 g, 3.4 mmol) and Et_3N (0.7 g, 7 mmol) in THF was added dropwise, while stirring, to a solution of 2,6-bis(chloromethyl)-4-methylphenol (0.35 g, 1.7 mmol) in THF. After refluxing for 2 h, the solution was cooled to room temperature. Filtration of the triethylammonium salt and subsequent evaporation of the solvent resulted in an oil, which was dissolved in acidified water and washed with dichloromethane. The water layer was made alkaline by adding a concentrated aqueous solution of NH_3, and the resulting suspension was extracted three times with dichloromethane. The combined organic layers were dried with Na_2SO_4 and the solvents evaporated under reduced pressure. The resulting oil was found to be the pure product. Yield: 0.77 g (84%). ^{1}H NMR ($CDCl_3$): δ = 2.28 (s, 3 H, CH_3), 3.82 (s, 4 H, NCH_2th), 3.85 (s, 4 H, phCH_2N), 3.89 (s, 4 H, NCH_2py), 6.95 (m, 4 H, 3′th + 4′th), 7.04 (s, 2 H, 3′ph + 5′ph), 7.15 (t, 2 H, 5′th), 7.24 (d, 2 H, 3′py), 7.53 (d, 2 H, 5′th), 7.66 (t, 2 H, 4′py), 8.56 (d, 2 H, 6′py), 10.40 (1 H, OH) ppm. ESI-MS: m/z = 541 [M + H$^+$].

[Cu_2(py2th2s)(μ-Cl)Cl_2]·CH_3OH (1): Hpy2th2s (0.15 g, 0.28 mmol) and copper chloride (0.10 g, 0.54 mmol) were dissolved in methanol (10 mL). Addition of diethyl ether (20 mL) resulted in the precipitation of the complex as a dark brown powder. Yield: 102 mg (46%). Single crystals of the complex were obtained by slow diffusion of diethyl ether into a 0.01 M solution of the complex. [Cu_2(symth2py2)Cl_3]·CH_3OH. $C_{32}H_{36}Cl_3Cu_2N_4O_2S_2$ (806.2): calcd. C 47.73, H 4.38, N 6.96, S 7.96; found C 45.73, H 4.14, N 7.25, S 7.91. ESI-MS: m/z = 737 [Cu_2(py2th2s)Cl_2]$^+$.

[Cu_2(py2th2s)(μ-Br)Br_2] (2): Hpy2th2s (0.15 g, 0.28 mmol) and copper bromide (0.12 g, 0.54 mmol) were dissolved in of methanol (10 mL). After addition of diethyl ether to the resulting solution, the complex precipitated as a dark purple crystalline powder. Yield: 155 mg (64%). Crystals suitable for X-ray diffraction were obtained by slow diffusion of diethyl ether into a 0.01 M solution of the complex in acetonitrile. $C_{31}H_{31}Br_3Cu_2N_4OS_2$ (906.5): calcd. C 40.95, H 3.76, N 5.97, S 6.83; found C 39.76, H 3.42, N 6.07, S 6.50. ESI-MS: m/z = 827 [Cu_2(py2th2s)Br_2]$^+$.

X-ray Structures

Compound 1: A single crystal of [Cu_2(py2th2s)(μ-Cl)Cl_2]·CH_3OH (**1**) was mounted at 150 K on a ᵇruker AXS SMART 6000 diffractometer, equipped with Cu-K_α radiation (λ = 1.54184 Å). $C_{32}H_{35}Cl_3Cu_2N_4O_2S_2$, M = 802.17, rectangular reddish-brown plate, 0.23 × 0.21 × 0.05 mm, a = 7.984(2) Å, b = 34.589(7) Å, c = 12.554(3) Å, β = 94.31(3)°, Z = 4, V = 3457(2) Å^3, $\rho_{calcd.}$ = 1.541 g·cm^{-3}, μ = 5.068 mm^{-1}, absorption correction with SADABS,[32] monoclinic, space group $P2_1/n$ (no. 14), 19864 reflections collected, 6317 independent reflections (R_{int} = 0.0386). The structure was solved by direct methods and refined using the SHELX program package.[33,34] All hydrogen atoms were placed on idealized positions riding on their carrier atoms with isotropic displacement parameters. The final cycle of full-matrix least-squares refinement, including 438 parameters, converted into $R1$ = 0.0352 ($R1$ = 0.0430 all data) and $wR2$ = 0.1009 ($wR2$ = 0.1038 all data) with a maximum (minimum) residual electron density of 0.535 (−0.466) e·Å^{-3}.

Compound 2: $C_{31}H_{31}Br_3Cu_2N_4OS_2$ + solvent, M = 906.53, red needle, 0.60 × 0.06 × 0.03 mm, triclinic, $P\bar{1}$ (no. 2), a = 8.4207(2) Å, b = 17.9812(4) Å, c = 24.2238(6) Å, α = 71.2709(9), β = 81.2708(7), γ = 80.6146(11)°, V = 3407.66(14) Å^3, Z = 4, $\rho_{calcd.}$ = 1.767 g·cm^{-3}, 43713 measured reflections, 12061 unique reflections (R_{int} = 0.0734), 8080 observed reflections [$I > 2\sigma(I)$], 775 refined parameters, no restraints; R (obsd. refl.): $R1$ = 0.0461, $wR2$ = 0.1121; R (all data): $R1$ = 0.0776, $wR2$ = 0.1286; S = 1.085; residual electron density between −1.08 and 1.17 e·Å^{-3}. Intensities were measured with a Nonius KappaCCD diffractometer with rotating anode (Mo-K_α, λ = 0.71073 Å) at a temperature of 150 K. An absorption correction based on multiple measured reflections was applied (μ = 4.920 mm^{-1}, 0.59−0.86 transmission). The structure was solved with direct methods with the program SHELXS-97,[35] and refined with the program SHELXL-97[34] against F^2 of all reflections up to a resolution of $(\sin/\lambda)_{max.}$ = 0.60 Å^{-1}. Non-hydrogen atoms were refined freely with anisotropic displacement parameters. Hydrogen atoms were refined as rigid groups. Three of the thiophene rings were rotationally disordered and refined with occupancies of 0.85:0.15, 0.72:0.28, and 0.55:0.45, respectively. The crystal structure contains large voids (150.9 Å^3/unit cell) filled with disordered solvent molecules. Their contribution to the structure factors was secured by back-Fourier transformation (program

PLATON,[17] CALC SQUEEZE; 22 e^-/unit cell). The drawings, structure calculations, and checking for higher symmetry was performed with the program PLATON.[17]

CCDC-230014 (**1**) and -230015 (**2**) contain the supplementary crystallographic data for this paper. These data can be obtained free of charge at www.ccdc.cam.ac.uk/conts/retrieving.html [or from the Cambridge Crystallographic Data Centre, 12 Union Road, Cambridge CB2 1EZ, UK; Fax: + 44-1223-336-033; E-mail: deposit@ccdc.cam.ac.uk].

Acknowledgments

Support from the NRSC Catalysis (a Research School Combination of HRSMC and NIOK) is kindly acknowledged. Also support and sponsorship from COST Action D21/003/2001 is kindly acknowledged. This project was financially supported by the Dutch Economy, Ecology, Technology (EET) program, a joint program of the Ministry of Economic Affairs, the Ministry of Education, Culture and Science, and the Ministry of Housing, Spatial Planning and the Environment. This work was supported in part (M. L., A. L. S.) by The Netherlands Foundation for Chemical Sciences (CW) with financial aid from the Netherlands Organization for Scientific Research (NWO).

[1] E. I. Solomon, U. M. Sundaram, T. E. Machonkin, *Chem. Rev.* **1996**, *96*, 2563−2605.
[2] T. Plenge, R. Dillinger, L. Santagostini, L. Casella, F. Tuczek, *Z. Anorg. Allg. Chem.* **2003**, *629*, 2258−2265.
[3] L. Santagostini, M. Gullotti, R. Pagliarin, E. Monzani, L. Casella, *Chem. Commun.* **2003**, *17*, 2186−2187.
[4] K. D. Karlin, J. C. Hayes, Y. Gultneh, R. W. Cruse, J. W. McKown, J. P. Hutchinson, J. Zubieta, *J. Am. Chem. Soc.* **1984**, *106*, 2121−2128.
[5] K. D. Karlin, T. Zoltan, A. Farooq, M. S. Haka, P. Ghosh, R. W. Cruse, Y. Gultneh, J. C. Hayes, P. J. Toscano, J. Zubieta, *Inorg. Chem.* **1992**, *31*, 1436−1451.
[6] J. Reim, B. Krebs, *J. Chem. Soc., Dalton Trans.* **1997**, 3793−3804.
[7] S. Torelli, C. Belle, S. Hamman, J. L. Pierre, E. Saint-Aman, *Inorg. Chem.* **2002**, *41*, 3983−3989.
[8] H. Börzel, P. Comba, H. Pritzkow, *Chem. Commun.* **2001**, 97−98.
[9] T. Klabunde, C. Eicken, J. C. Sacchettini, B. Krebs, *Nat. Struct. Biol.* **1998**, *5*, 1084−1090.
[10] C. Eicken, B. Krebs, J. C. Sacchettini, *Curr. Opin. Struct. Biol.* **1999**, *9*, 677−683.
[11] S. Torelli, C. Belle, I. Gautier-Luneau, J. L. Pierre, E. Saint-Aman, J. M. Latour, L. Le Pape, D. Luneau, *Inorg. Chem.* **2000**, *39*, 3526−3536.
[12] M. Thirumavalavan, P. Akilan, M. Kandaswamy, Kandaswamy Chinnakali, G. Senthil Kumar, H. K. Fun, *Inorg. Chem.* **2003**, *42*, 3308−3317.
[13] M. E. Cuff, K. I. Miller, K. E. van Holde, W. A. Hendrickson, *J. Mol. Biol.* **1998**, *278*, 855−870.
[14] C. Gielens, N. de Geest, X. Q. Xin, B. Devreese, J. van Beeumen, G. Preaux, *Eur. J. Biochem.* **1997**, *248*, 879−888.
[15] K. Lerch, *J. Biol. Chem.* **1982**, *257*, 6414−6419.
[16] A. S. Borovik, V. Papaefthymiou, L. F. Taylor, O. P. Anderson, L. Que, *J. Am. Chem. Soc.* **1989**, *111*, 6183−6195.
[17] A. L. Spek, *J. Appl. Crystallogr.* **2003**, *36*, 7−13.
[18] A. W. Addison, T. N. Rao, J. Reedijk, J. van Rijn, G. C. Verschoor, *J. Chem. Soc., Dalton Trans.* **1984**, 1349−1356.
[19] U. Rajendran, R. Viswanathan, M. Palaniandavas, N. Laskiminaraya, *J. Chem. Soc., Dalton Trans.* **1994**, 1219−1226.
[20] E. Ruiz, P. Alemany, S. Alvarez, J. Cano, *J. Am. Chem. Soc.* **1997**, *119*, 1297−1303.
[21] K. Bertoncello, G. D. Fallon, J. H. Hodgkin, K. S. Murray, *Inorg. Chem.* **1988**, *27*, 4750−4758.
[22] T. N. Sorrel, C. J. O′Connor, O. P. Anderson, J. H. Reibenspies, *J. Am. Chem. Soc.* **1985**, *107*, 4199−4206.
[23] C. Belle, C. Beguin, I. Gautier-Luneau, S. Hamman, C. Philouze, J. L. Pierre, F. Thomas, S. Torelli, E. Saint-Aman, M. Bonin, *Inorg. Chem.* **2002**, *41*, 479−491.
[24] W. J. Geary, *Coord. Chem. Rev.* **1971**, *7*, 81−122.
[25] R. A. Walton, *Quart. Rev.* **1965**, *19*, 126−143.
[26] K. D. Karlin, Y. Gultneh, T. Nicholson, J. Zubieta, *Inorg. Chem.* **1985**, *24*, 3725−3727.
[27] C. Fernandes, A. Neves, A. J. Bortoluzzi, A. S. Mangrich, E. Rentschler, B. Szpoganicz, E. Schwingel, *Inorg. Chim. Acta* **2001**, *320*, 12−21.
[28] C.-H. Kao, H.-H. Wei, Y.-H. Liu, G.-H. Lee, Y. Wang, C.-J. Lee, *J. Inorg. Biochem.* **2001**, *84*, 171−178.
[29] A. Neves, L. M. Rossi, A. J. Bortoluzzi, B. Szpoganicz, C. Wiezbicki, E. Schwingel, W. Haase, S. Ostrovsky, *Inorg. Chem.* **2002**, *41*, 1788−1794.
[30] J. Mukherjee, R. Mukherjee, *Inorg. Chim. Acta* **2002**, *337*, 429−438.
[31] I. M. Kolthoff, P. J. Elving, *Treatise on Analytical Chemistry*, Interscience Encyclopedia, Inc., New York, **1963**, vol. 4.
[32] *SAINT Plus V 6.02*, Bruker AXS, Inc., Madison, WI, **1999**.
[33] G. M. Sheldrick, *SHELXTL PLUS*, University of Göttingen, Germany, **1990**.
[34] G. M. Sheldrick, *SHELXL-97, Program for the refinement of crystal structures*, University of Göttingen, Germany, **1997**.
[35] G. M. Sheldrick, *SHELXS-97, Program for crystal structure solution*, University of Göttingen, Germany, **1997**.

Received February 4, 2004
Early View Article
Published Online August 17, 2004

